

Article

Characterization, Antioxidant and Cytotoxic Evaluation of Demethoxycurcumin and Bisdemethoxycurcumin from *Curcuma longa* Cultivated in Costa Rica

Andrea Mariela Araya-Sibaja ^{1,*} , Felipe Vargas-Huertas ² , Silvia Quesada ³ , Gabriela Azofeifa ³ ,
José Roberto Vega-Baudrit ¹  and Mirtha Navarro-Hoyos ² 

¹ Laboratorio Nacional de Nanotecnología, LANOTEC-CeNAT-CONARE, Pavas, San José 1174-1200, Costa Rica; jvegab@gmail.com

² Laboratorio BIODISS, Escuela de Química, Universidad de Costa Rica, San Pedro de Montes de Oca, San José 2060, Costa Rica; luis.vargashuertas@ucr.ac.cr (F.V.-H.); mnavarro@codeti.org (M.N.-H.)

³ Departamento de Bioquímica, Escuela de Medicina, Universidad de Costa Rica, San Pedro de Montes de Oca, San José 2060, Costa Rica; silvia.quesada@ucr.ac.cr (S.Q.); gabriela.azofeifacordero@ucr.ac.cr (G.A.)

* Correspondence: aaraya@cenat.ac.cr; Tel.: +506-2519-5700 (ext. 6016)

Abstract: The biological activities of curcuminoids, the main polyphenol constituents of *Curcuma longa* (turmeric), have been the subject of many studies in recent years. However, these studies have focused on the major active compound, curcumin (CUR), while other important constituents, demethoxycurcumin (DMC) and bisdemethoxycurcumin (BDM) have been less studied and reported in the literature regarding their bioactivity as well as their isolation and solid-state characterization. Hence, in this study, DMC and BDM were isolated using pressurized liquid extraction (PLE) followed by column chromatography and crystallization. HRMS and ¹H and ¹³C NMR were used to characterize them. Solid-state characterization was performed through powder X-ray diffraction (PXRD), Fourier transform infrared spectroscopy (FT-IR), differential scanning calorimetry (DSC), and scanning electron microscopy (SEM) techniques. Further, powder dissolution profiles were performed in two media, antioxidant and cytotoxic activities were determined through 2,2-diphenyl-1-picrylhydrazyl (DPPH) and an MTT assay on gastric adenocarcinoma (AGS), colorectal adenocarcinoma (SW-620), and hepatocellular carcinoma (HepG2) cell lines. DMC and BDM were extracted from *Curcuma longa* cultivated in Costa Rica, using pressurized liquid extraction (PLE), then isolated and purified, combining column chromatography and crystallization techniques. The highly pure solids obtained were shown to be crystalline with an amorphous component. Although the PXRD pattern of BDM suggested a high amorphous component, the crystal exhibited a well-defined and faceted shape. Meanwhile, DMC crystallized in a botryoidal habit, and this constitutes the first report for this compound. On the other hand, BDM was slightly more soluble than DMC, which in turn showed an antioxidant IC₅₀ value 28% higher than BDM (12.46 and 17.94 µg/mL, respectively). In respect to the cytotoxic effects, DMC showed a better IC₅₀ value than BDM for both the SW-620 and AGS cell lines, while BDM exhibited a better IC₅₀ value than DMC against the HepG2 cell line (64.7 µM). In terms of selectivity, BDM and DMC had the highest SI value for SW-620 cells compared to non-tumoral cells, while both compounds also displayed the best cytotoxic effect against these colon adenocarcinoma SW-620 cells, indicating BDM and DMC as potential chemotherapeutic drugs.

Keywords: *Curcuma longa*; demethoxycurcumin; bisdemethoxycurcumin; dissolution profile; DPPH; MTT



Citation: Araya-Sibaja, A.M.; Vargas-Huertas, F.; Quesada, S.; Azofeifa, G.; Vega-Baudrit, J.R.; Navarro-Hoyos, M. Characterization, Antioxidant and Cytotoxic Evaluation of Demethoxycurcumin and Bisdemethoxycurcumin from *Curcuma longa* Cultivated in Costa Rica. *Separations* **2024**, *11*, 23. <https://doi.org/10.3390/separations11010023>

Academic Editor: Paraskevas D. Tzanavaras

Received: 14 November 2023

Revised: 23 December 2023

Accepted: 31 December 2023

Published: 8 January 2024



Copyright: © 2024 by the authors. Licensee MDPI, Basel, Switzerland. This article is an open access article distributed under the terms and conditions of the Creative Commons Attribution (CC BY) license (<https://creativecommons.org/licenses/by/4.0/>).

1. Introduction

Polyphenols are natural compounds, of interest in the human diet due to their recognized beneficial properties for health [1]. Curcuminoids are the main polyphenol constituents of the rhizomes from *Curcuma longa* (*C. longa*), usually known as turmeric. Curcumin (CUR) constitutes the major active compound, whose content is around 65–80%,

while other important constituents are demethoxycurcumin (DMC), with 12–17%, and bisdemethoxycurcumin (BDM), with 3–7% [2,3].

In recent years, curcuminoids have been the subject of studies of their biological activities [4] including antiulcer, antifibrotic, antiviral, antibacterial, antiprotozoal, antimutagenic, antifertility, antidiabetic, anticoagulant, antivenom, antioxidant, antihypertensive, antihypercholesterolemic, and anticancer [4], among others. Nevertheless, special attention has been given to CUR, which has been intensively explored through in vivo and in vitro studies, confirming that CUR regulates a wide range of immune system responses [5,6] and modulates the production and activity of different cytokines and interferons, key proteins that play an important role in diseases related to immunological alterations, such as cancer [7–9]. The growing interest in this compound led to several reports focused on isolating, characterizing, and evaluating the bioactivity of CUR, while for DMC and BDM the literature is less abundant.

Considering the similarity in the CUR, DMC, and BDM chemical structures shown in Figure 2, it would be expected that DMC and BDM would display analogous bioactivities and pharmacological effects [10]. In fact, there are some reports studying the anti-inflammatory, antioxidant, anticancer and, pro-apoptotic activities properties of DMC and BDM [11,12]. Indeed, it has been reported that BDM has greater potency against the invasion of cancer cells, by cleavage of the extracellular matrix, than CUR [13].

Although CUR has a wide range of pharmacological activity, its pharmacokinetic deficiency has been observed through many in vivo studies failing several preclinical and clinical studies, thus limiting its applicability and approval as a drug in the treatment of diseases [14,15]. However, DMC and BDM have been reported to possess more stable chemical characteristics compare to CUR, hence they are promising as drug substances [16] and should be further investigated not only in terms of their bioactivities but also in terms of methods to isolate them and to perform solid-state characterization. Hence, in this contribution, DMC and BDM were extracted and isolated from *C. longa* rhizomes cultivated in Costa Rica, as well as identified chemically and structurally. Further, their dissolution profiles, as well as antioxidant and cytotoxic activities, were evaluated. The results reported herein are valuable and constitute an essential component in the separation and characterization processes of potential active pharmaceutical ingredients.

2. Materials and Methods

2.1. Materials, Reagents, and Solvents

Rhizomes from *C. longa* were acquired from a producer in the northern region from Costa Rica. They were cleansed with water, chopped into fine slices, and dried in an oven at 40 °C, until reaching constant weight. The dried material was ground and preserved in sealed containers at −20 °C until extraction. DMC and BDM analytical standards for quantification, 2,2-diphenyl-1-picrylhydrazyl (DPPH), phosphoric acid (H₃PO₄), disodium hydrogen phosphate, and sodium dihydrogen phosphate monohydrate were purchased from Sigma–Aldrich (Burlington, MA, USA). Chloroform (CHCl₃), isopropanol (IPA), methanol (MeOH), and acetonitrile (MeCN) and acetone were purchased from JTBaker (Phillipsburg, NJ, USA). All solvents were HPLC/UV-grade or highly pure, and the water was purified using a Millipore system filtered through a Millipore membrane 0.22 µm Millipak 40. Finally, the human gastric adenocarcinoma cell line AGS, human colorectal adenocarcinoma SW-620, and HepG2 human hepatocellular carcinoma, were obtained from the American Type Culture Collection (ATCC, Rockville, MD, USA).

2.2. Extraction of Curcuminoids

The extraction of curcuminoids was carried out through a previously optimized pressurized liquid extraction (PLE) method [17]. The PLE equipment used was a Dionex™ ASE™300 accelerated solvent extractor (Thermo Scientific™, Waltham, MA, USA). For each extraction, 7.5 g of turmeric powder was inserted into a 34 mL cell and extracted using a method consisting of 3 cycles of 10 min static time each, at a temperature of 80 °C, using acetone as

solvent. The extracts were dried out using a Buchi™215 (Flawil, Switzerland) rotavapor and the extraction yield was determined. UPLC-DAD quantification for the three main curcuminoids was carried out according to the chromatographic method described below.

The chromatographic analysis was carried out in a UHPLC U3000 Thermo Scientific with a DAD detector. Chromatographic separation was performed using a Luna RP-C18 column (150 mm × 4.6 mm i.d. × 4 μm, Phenomenex, Torrance, CA, USA) with a pre-column filter (Phenomenex, Torrance, CA, USA). The mobile phase consisted of water (A), MeOH (B), and MeCN (C). An isocratic method was used with 45% A, 15% B, and 40% C, and detection was carried out at 420 nm.

2.3. Identification of Curcuminoids by UHPLC-MS

The three main curcuminoids, CUR, DMC, and BDM were identified using a Thermo Scientific MSQ Plus detector, using a negative mode ESI ionizer, with an ESI temperature of 550 °C, cone voltage set to 70 V, and needle voltage to 3 kV. The three signals corresponding to each of the three curcuminoids were observed, the first with a lower R_t and 307 m/z corresponding to BDM, followed by a peak with 337 m/z corresponding to DMC, and finally a signal with higher R_t and 367 m/z corresponding to CUR.

2.4. Isolation of BDM and DMC

The isolation of the curcuminoids was performed from extracts obtained using the optimized PLE method, starting with 7.5 g of dried turmeric as previously described, through column chromatography. The column was prepared using Sigma Aldrich silica (Silica gel 60 Merck Millipore 70–230 mesh) with the dimensions of the column being 3.5 cm in diameter and 30 cm in height and an elution gradient consisting of 100% CHCl₃, followed by mixtures of CHCl₃: MeOH of 99:1, 98:2, 97:3, 96:4, 95:5, 93:7, 90:10, and 100% methanol. Fractions were collected and grouped according to thin-layer chromatography (TLC) analysis.

2.5. NMR Characterization of Purified BDM and DMC

The isolated curcuminoids, BDM and DMC, were characterized by ¹H and ¹³C NMR. A mass of 10 mg of each were weighed and dissolved in 750 uL of methanol-d₄. The measurements were performed on a 400 MHz Bruker instrument.

2.6. Solid-State Characterization of DMC and BDM

2.6.1. Powder X-ray Diffraction

The PXRD analyses were conducted in a PANalytical Empyrean diffractometer (Malvern Panalytical, Malvern, UK) with a copper tube ($\lambda=1.54 \text{ \AA}$), using a PIXcel detector (Medipix2). A soller of 0.04 rad positioned at the X-ray tube and a large soller of 0.04 rad placed at the detector were used. A divergence slit of 1/4° and antiscatter slit of 1/2° were employed. K β was filtered using Nickel. Samples were placed in a zero-background sample holder and scanned from 4° to 40° using 45 kV and 40 mA. The software Data Collector, High Score plus (version 5.1), and PDF4+ (2021) were utilized.

2.6.2. Fourier Transform Infrared Spectroscopy (FT-IR)

FT-IR spectra were collected using 32 scans at a resolution of 4 cm⁻¹ from a Thermo Scientific Nicolet iS50 spectroscope. The instrument was equipped with a diamond attenuated total reflectance (ATR) accessory. The samples were positioned directly into the ATR device and measured in the range of 4000–600 cm⁻¹, collecting 32 scans at a resolution of 4 cm⁻¹.

2.6.3. Differential Scanning Calorimetry (DSC)

DSC curves of the samples were measured in a TA Instruments DSC-Q200 calorimeter provided with a TA Refrigerated Cooling System 90 (TA Instrument, New Castle, DE, USA). An appropriate amount of sample (between 2 and 5 mg) was deposited in an aluminum pan

with a lid and measured under a dynamic nitrogen atmosphere of 50 mL/min, a heating rate of 10 °C/min, and a temperature range from 40 to 250 °C.

2.6.4. Scanning Electron Microscopy

The morphology and crystal size of BDM and DMC were observed using a JEOL JSM-6390 LV scanning electron microscope (JEOL USA, Inc., Peabody, MA, USA), using an acceleration voltage of 20 kV. The samples were mounted on metal stubs using double-sided adhesive tape and coated with gold under vacuum in an argon atmosphere.

2.7. *In Vitro* Studies

2.7.1. Powder Dissolution Test

The dissolution tests of BDM and DMC powder samples were performed using the United States Pharmacopeia (USP) paddle method on a SOTAX S7 dissolution test system. Two dissolution media were tested, a phosphate-buffered saline (pH 7.4) and water (pH 6.8). Each media was previously heated at 37 ± 0.5 °C, and the rotation speed was 100 rpm, as indicated in the USP method. At specific time intervals, 5 mL of the sample was withdrawn, and the medium was replaced with the same volume of preheated fresh medium to ensure sink conditions. The removed sample was filtered using a 0.45 µm cellulose acetate membrane put into a Sartorius stainless-steel syringe filter holder and the BDM and DMC concentrations, without further dilution in organic solvents, were determined. The assessment was conducted in triplicate.

The individual curcuminoid content was determined using a Thermo Scientific™ Ultimate™ 3000 UHPLC system equipped with a variable wavelength detector, pump, variable temperature compartment column, and an autosampler. The chromatographic separation of BDM and DMC was achieved using a Nucleosil 100-5C18 column (250 mm × 4.0 mm, 5 µm packing) with a 1.0 mL/min rate flow, maintained at 37.5 °C. The mobile phase was composed of acetonitrile: phosphoric acid 0.1%, using a gradient elution starting at 45:55 to reach 65:35 in 20 min. The detection and quantification were performed at 420 nm.

2.7.2. DPPH Radical-Scavenging Activity

A DPPH evaluation of BDM and DMC was conducted as reported previously [17]. In brief, a solution of 2,2-diphenyl-1-picrylhydrazyl (DPPH) (0.25 mM) was set in ethanol. A volume of 0.5 mL of this solution was mixed with 1 mL of the sample under evaluation at different concentrations and incubated at 25° C in the dark for 30 min. The DPPH absorbance was measured at 517 nm. Blanks were prepared for each concentration and the DPPH absorbance was measured at 517 nm. The inhibition percentage was determined as shown in Equation (1):

$$\text{Inhibition percentage(\%)} = \frac{(Abs_{blank} - Abs_{sample})}{Abs_{blank}} * 100 \quad (1)$$

The percentage of the radical-scavenging activity of the sample was plotted against its concentration to calculate the IC₅₀, which corresponds to the amount of sample necessary to reach a 50% radical-scavenging activity. Each sample was analyzed in three independent assays.

2.7.3. Cytotoxicity assessment on tumoral cells

Cell Culture

Three different human cancer cell lines, namely, gastric AGS, colorectal SW-620, and hepatocellular HepG2 cells, as well as monkey normal Vero kidney cells, were used. Minimum essential Eagle's medium (MEM), holding 10% fetal bovine serum (FBS), served to grow these four cell types, along with amphotericin B (0.25 µg/mL), penicillin (100 IUmL⁻¹), glutamine (2 mmol/L) and streptomycin (100 µg/mL). A humidified atmosphere at a temperature of 37 °C with 5% CO₂ was used. Cells were sub-cultured using a trypsin-EDTA

solution for detachment, with a confluence of around 70–80%. Once growth was achieved, a volume of 100 μL of cell suspension (1.5×10^5 cells/mL) was seeded into 96-well plates overnight. Subsequently, different concentrations of curcuminoids in volumes of 50 μL each, were added to the seeded cells and cell culture medium was added to obtain final concentrations from 15 to 500 $\mu\text{g}/\text{mL}$, then left in incubation for 48 h. A similar procedure was used to prepare control cultures, which were achieved by not adding any curcuminoids to the cultured cells.

Cytotoxicity Evaluation through MTT Assay

A cytotoxicity assessment for each curcuminoid sample was achieved through the measurement of the level of MTT reaction with available cells, since a sample's cytotoxicity towards cells leads to a decrease in their viability. After the 48 h incubation, the cells' medium was removed, and PBS ($2 \times 100 \mu\text{L}$) was used to wash the cells. Subsequently, an MTT solution in culture medium (5 mg/mL) was added (100 μL) and the mixture was left for incubation at 37 °C for 2 h. Afterwards, 95% ethanol was added (100 μL) to dissolve the formazan crystals and the plates were put in a microplate reader to measure the absorbance at a wavelength of 570 nm. Dose–response curves were established for each sample and concentration and, finally, the cell viability reduction by 50%, or IC_{50} , was calculated from these curves.

3. Results and Discussion

3.1. Isolation and Purification of BDM and DMC

A chromatographic column was prepared employing silica as the stationary phase and an elution gradient of $\text{CHCl}_3:\text{MeOH}$ as the mobile phase; the specific conditions are detailed in the corresponding experimental section. The crude extract was obtained through the optimized PLE method to obtain a crude extract with 17.6% yield/dry g, as indicated in the Materials and Methods section. From the 40 fractions obtained, fractions 13 to 16 corresponded to DMC, with a mass of 101.2 mg, and fractions 18 to 22 corresponded to BDM, with a mass of 307.6 mg, while CUR was obtained in fractions 9 to 12 with a mass of 1088.4 mg. The total mass of the isolated curcuminoids corresponded to a 56.7% extraction yield, and a 7.2% dry mass yield.

The UPLC-DAD analyses indicated purities of 98% for both BDM and DMC and the chromatograms are shown in Figure 1. In MS, $[\text{M}+\text{H}]^+$ ions at m/z 309.1137, 339.1262, and 369.1358 were obtained for BDM, DMC, and CUR, respectively, as previously reported [17], and characteristic fragments were found at m/z 177, for CUR and DMC, as well as at m/z 147 for BDM and DMC, corresponding to cleavages between the C3–C4 and C4–C5 bonds, as shown in Figure 2.

Further, the results of the NMR analysis confirmed the isolation and purification of each curcuminoid, whose structures are presented in Figure 2. The ^1H - and ^{13}C -NMR spectra are shown in Figure 3.

The signals for the ^1H -NMR and ^{13}C -NMR spectra of purified curcumin are summarized in Table 1 and are in agreement with the literature [18]. The peaks observed at 56.46 ppm and 184.76 ppm in the ^{13}C -NMR spectrum correspond to the methoxy and carbonyl groups, respectively, and a singlet corresponding to methoxy groups is observed at 3.94 ppm in the ^1H -NMR spectrum.

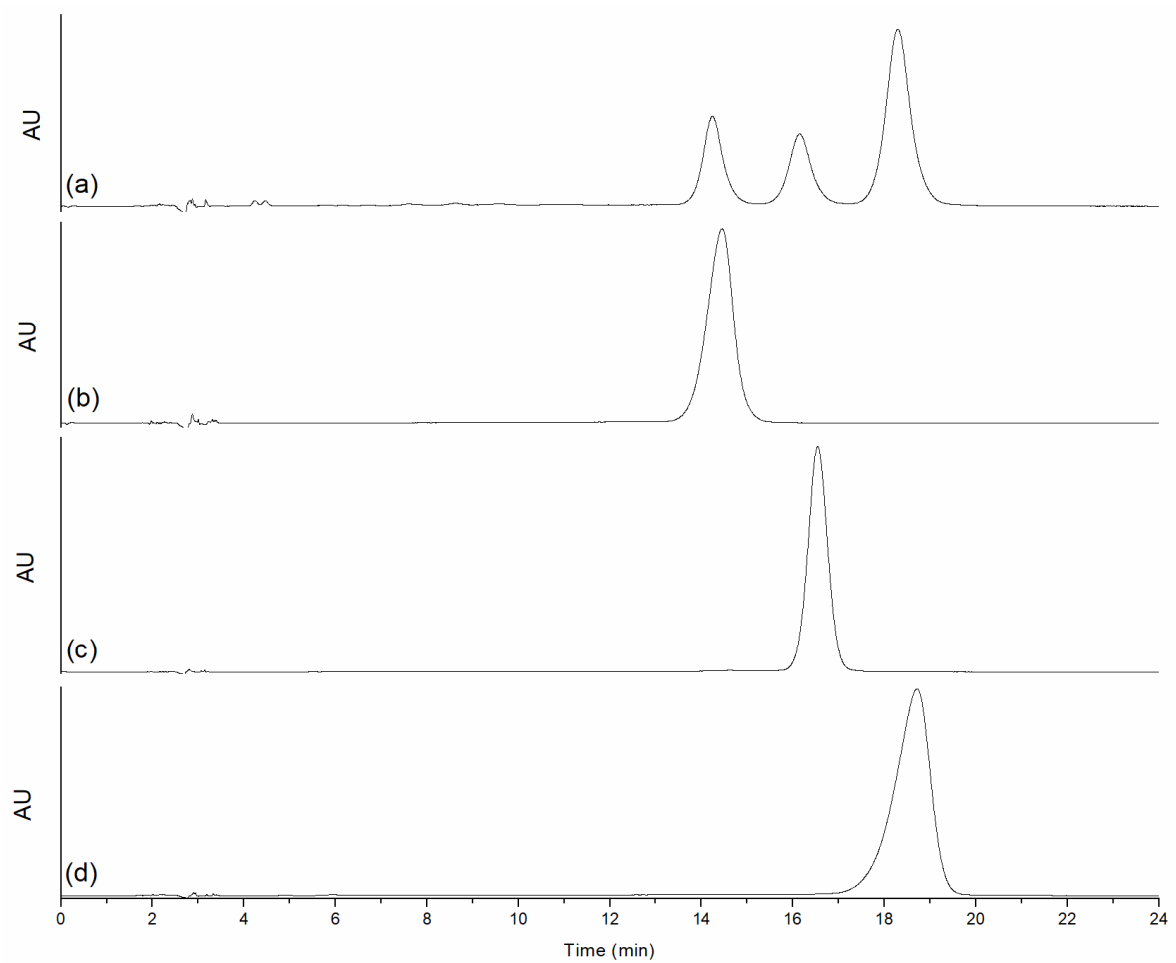


Figure 1. Chromatograms of (a) the three curcuminoids, (b) BDM, (c) DMC, (d) CUR.

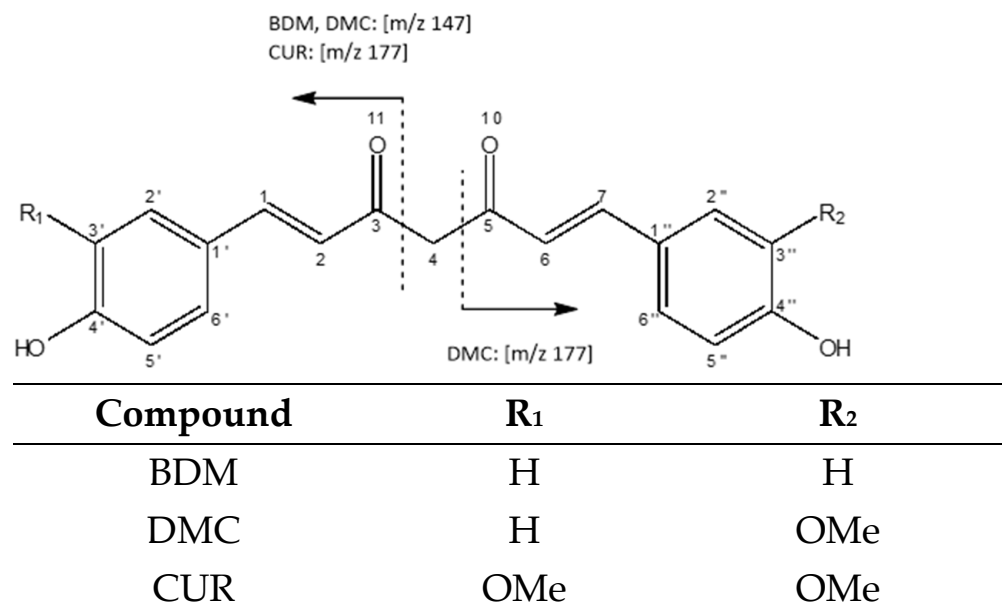


Figure 2. Structure of isolated curcuminoids.

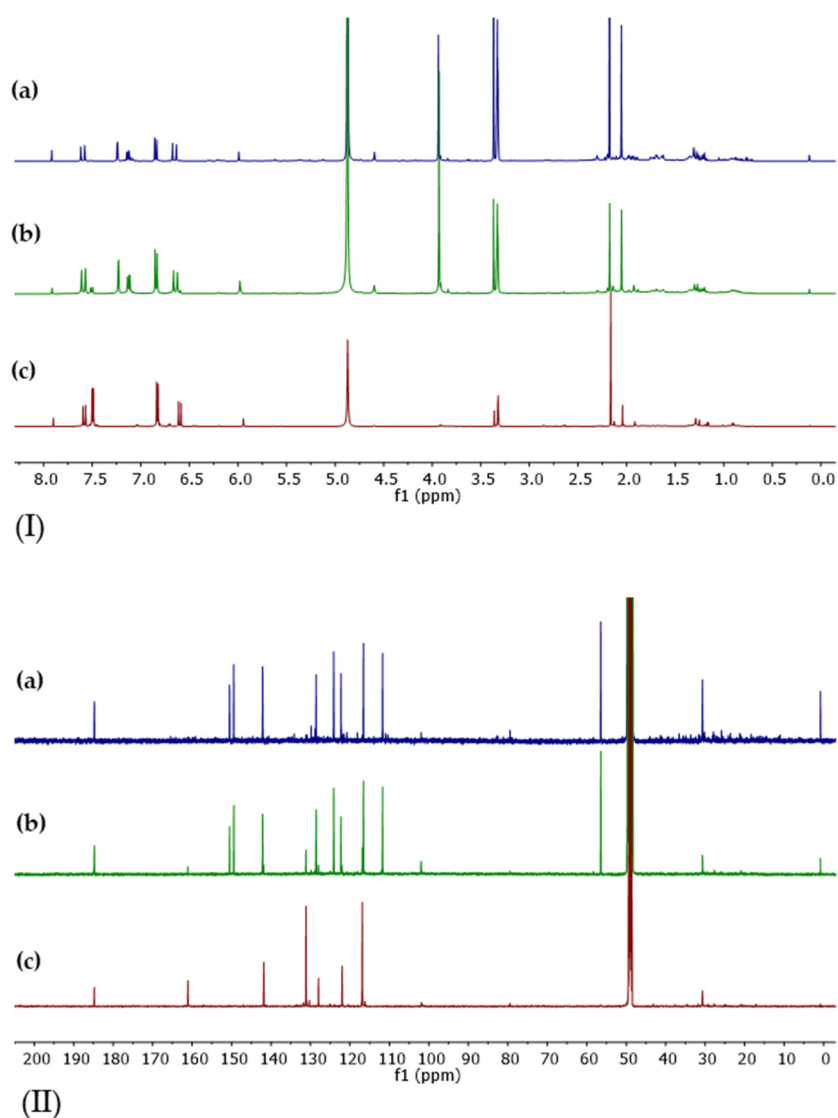


Figure 3. Spectra (I) $^1\text{H-NMR}$ and (II) $^{13}\text{C-NMR}$ for isolated curcuminoids: (a) CUR, (b) DMC, and (c) BDM. The measurements were made on a 400 MHz Bruker instrument.

Table 1. $^1\text{H-}$ and $^{13}\text{C-NMR}$ (methanol- d_4) signals for isolated CUR.

# C	^{13}C (ppm)	^1H (ppm)
3, 5	184.76	
4', 4''	150.49	
3', 3''	149.43	
1, 7	142.14	7.60 (d, $J = 15.8$ Hz, 2 H)
1', 1''	128.58	
6', 6''	124.13	7.13 (dd, $J = 8.2, 1.9$ Hz, 2 H)
2, 6	122.26	6.65 (d, $J = 15.8$ Hz, 2 H)
5', 5''	116.57	6.85 (d, $J = 8.2$ Hz, 2 H)
2', 2''	111.72	7.24 (d, $J = 1.9$ Hz, 2 H)
4	101.98	5.99 (s, 2 H)
(C3', C3'')-O-CH ₃	56.46	3.94 (s, 6 Hh)

As for the aromatic signals, a splitting pattern coinciding with the 1,3,4-trisubstituted ring is shown, as evidenced by the signal at 6.85 ppm ($\text{H}5'$, $\text{H}5''$), which shows a splitting with $J = 8.2$ ppm, consistent with a coupling with the *ortho* proton at 7.13 ppm ($\text{H}6'$, $\text{H}6''$).

This latter is observed as a doublet of doublets, with a second splitting of $J = 1.9$ Hz due to the coupling with the protons in *meta* position (7.24 ppm, H2' and H2'').

On the other hand, the NMR signals for BDM are presented in Table 2. Distinctively, the absence of the methoxy signals is observed in the ^{13}C -NMR spectrum, as well as the presence of signals that correspond to a *para*-substituted aromatic system at 116.88 ppm and 131.14 ppm, which also results in a lower number of carbon signals in the olefin region, as well as the displacement of the peaks of C4'' and C4'' from 150.49 ppm in CUR to 161.06 ppm in BDM.

Table 2. ^1H - and ^{13}C -NMR (methanol- d_4) signals from isolated BDM.

# C	^{13}C (ppm)	^1H (ppm)
3, 5	184.79	
4', 4''	161.06	
1, 7	141.84	7.58 (d, $J = 15.8$ Hz, 2 H)
2', 2'', 6', 6''	131.14	7.49 (d, $J = 8.6$ Hz, 4 H)
1', 1''	127.99	
2, 6	121.97	6.60 (d, $J = 15.8$ Hz, 2 H)
3', 3'', 5', 5''	116.88	6.83 (d, $J = 8.6$ Hz, 4 H)
4	101.88	5.94 (s, 2 H)

In the ^1H -NMR spectrum, the most significant change, in addition to the absence of methoxy signals, is observed in the aromatic region, with the disappearance of signals at 7.13 ppm and 7.24 ppm, which are replaced by a doublet at 7.49 ppm that is part of the *p*-substituted system along with the peak at 6.83 ppm, with a coupling constant $J = 8.6$ Hz, as they are adjacent protons in the aromatic ring.

Finally, the ^1H - and ^{13}C -NMR spectra for DMC are summarized in Table 3, where a greater number of signals can be observed in both spectra due to the loss of symmetry in the molecule.

Table 3. ^1H - and ^{13}C -NMR signals (methanol- d_4) of isolated DMC.

# C	^{13}C (ppm)	^1H (ppm)
5	184.81	
3	184.76	
4'	161.09	
4''	150.47	
3''	149.42	
1, 7	142.13	7.59 (d, $J = 15.8$ Hz)
2', 6'	131.5	7.51 (d, 8.7 Hz)
1''	128.58	
1'	127.99	
6''	124.12	7.12 (dd, $J = 8.2, 1.9$ Hz)
6	122.29	6.64 (d, $J = 15.8$ Hz)
2	122.25	6.61 (d, $J = 15.6$ Hz)
5''	116.89	6.84 (d, $J = 8.2$ Hz)
3', 5'	116.57	6.84 (d, $J = 8.2$ Hz)
2''	111.73	7.23 (d, $J = 1.9$ Hz)
4	102.00	5.98 (s)
(C3'')-O-CH ₃	56.45	3.93 (s)

The peaks coincide in shifts and multiplicity with either CUR or BDM, because one of the aromatic rings possesses a methoxy group similar to CUR, showing the respective signals, and the other aromatic moiety has an absence of a methoxy group and a *para*-substituted aromatic ring, similar to BDM. The spectra for the three curcuminoids coincide with those reported in the literature [19,20].

3.2. Solid-State Characterization of BDM and DMC

The crystal structure of BDM is reported in the Cambridge Structure Database (CSD) with the CSD entry XIWCUE. BDM crystallizes as monoclinic in the space group $P2/c$ with the cell parameters $a = 17.059(7) \text{ \AA}$, $b = 7.072(3) \text{ \AA}$, $c = 24.690(10)$, $\beta = 93.89(3)^\circ$, $\delta = \gamma = 90^\circ$ [21]. In addition, three other entries related to BDM are found in the CSD, being BUWKUZ01, XIWDAL, and XIWDEP, methanol, acetone, and propan-2-ol solvates, respectively. The experimentally derived BDM powder diffraction pattern compared to the calculated pattern from the CSD entry XIWCUE is presented in Figure 4A. There are only a few weak reflections observed in the BDM pattern, most of them are coincident with the calculated BDM pattern. However, the reflections around 24 and 29 degrees 2 theta are related with the acetone solvate [21] that could be obtained during the final recrystallization process. In addition, an important amorphous content in the material can be observed.

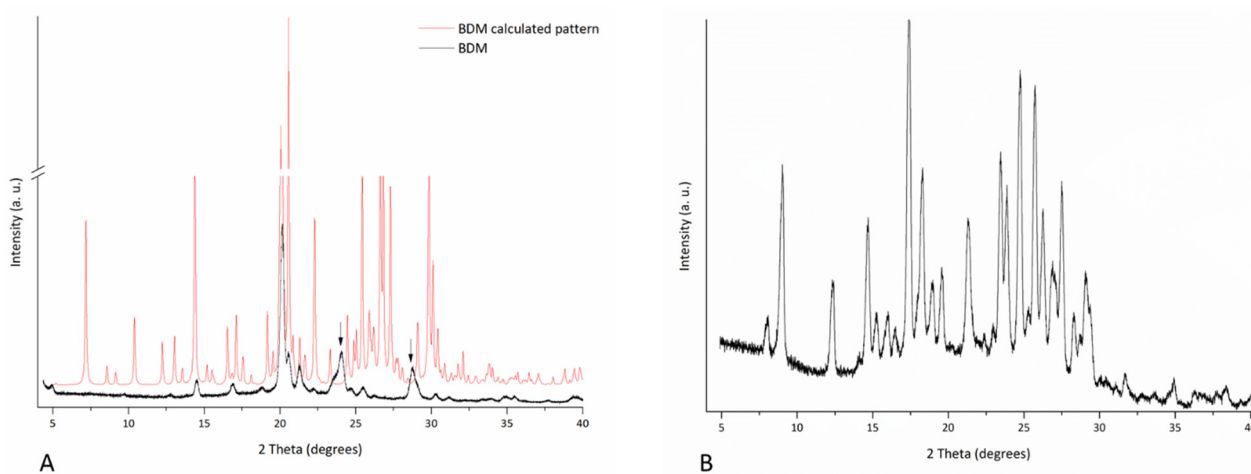
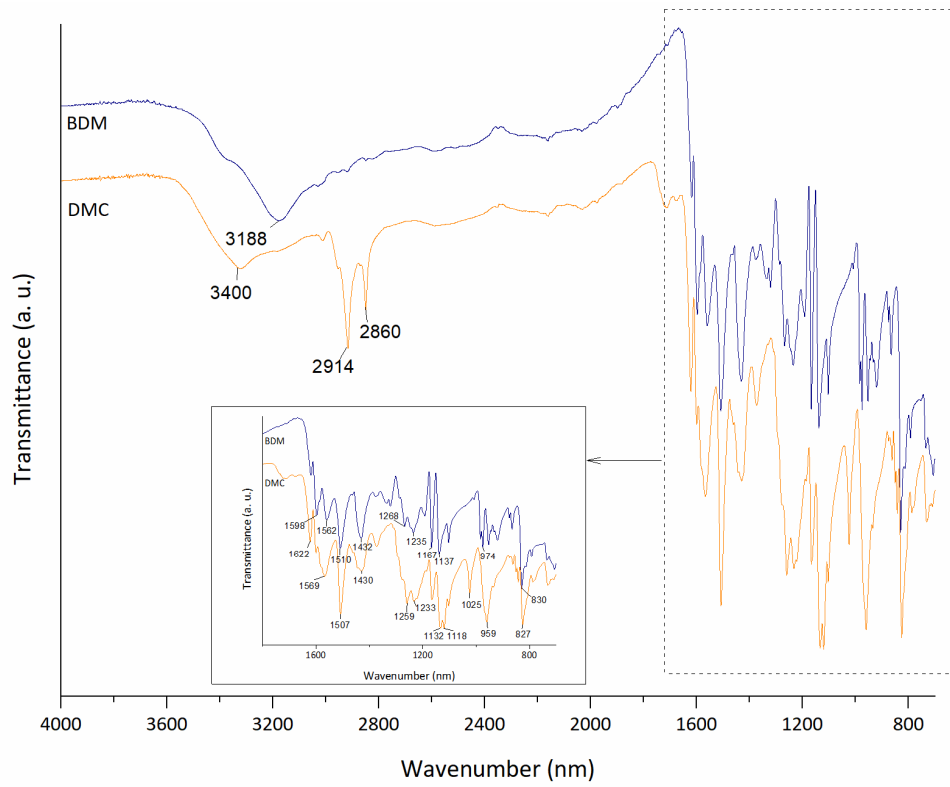


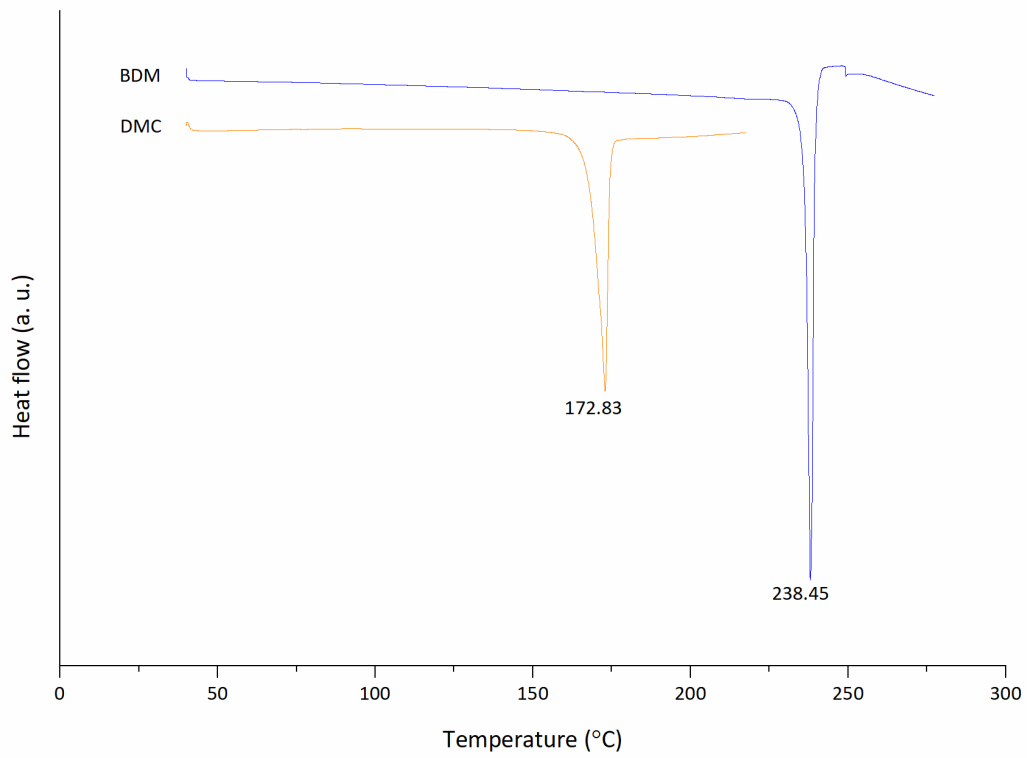
Figure 4. Experimental PXRD pattern of (A) BDM with the calculated pattern and (B) DMC.

On the other hand, DMC's crystal structure was not found either in the CCD or in the Crystallography Open Database (COD). Figure 4B shows the experimental DMC powder pattern, showing several reflections of medium intensity and a halo evidencing the presence of amorphous content.

The FT-IR spectra of BDM and DMC are shown in Figure 5A, in which characteristic peaks of curcuminoids associated with the stretching vibration of hydrogen-bonded -OH of phenolic hydroxyl groups at around 3400 and 3188 cm^{-1} in DMC and BDM, respectively, can be observed, consistent with the literature [22]. Sharp peaks at 2914 and 2860 cm^{-1} were observed only in DMC, corresponding to -C-H methyl asymmetric and symmetric stretching, respectively, which is consistent with the lack of methoxy groups in BDM. Other important bands were observed at 1622 cm^{-1} and 1569 cm^{-1} as well as at 1598 cm^{-1} and 1562 cm^{-1} , corresponding to the stretching vibration of the conjugated carbonyl (C=O) group for DMC and BDM, respectively [23]. Bands at 1507 cm^{-1} and 1510 cm^{-1} correspond to aromatic C-C stretching and at 1430 cm^{-1} and 1432 cm^{-1} are due to in-plane O-H deformation, for DMC and BDM, respectively. In turn, peaks at 1374 cm^{-1} and 1347 cm^{-1} correspond to -CH₂ scissoring, and bands at 1259 cm^{-1} and 1233 cm^{-1} (DMC), as well as at 1268 cm^{-1} and 1235 cm^{-1} (BDM), are due to C-O stretching. Finally, signals at 1132 cm^{-1} and 1137 cm^{-1} correspond to C-H in-plane deformation, and bands at 959 cm^{-1} and 974 cm^{-1} are due to -CH₂ out-of-plane bending for DMC and BDM, respectively [23].



A



B

Figure 5. Comparative (A) FT-IR spectra and (B) DSC curves for curcuminoids BDM and DMC.

The DSC curves of BDM and DMC are shown in Figure 5B. DMC and BDM exhibited singular endothermic events at 173 °C and 238 °C, respectively, aligned with values found in the literature [2,24].

The crystal morphology and sizes of both curcuminoids were observed by SEM images presented in Figure 6. BDM exhibited a well-defined and faceted prismatic-like crystal shape with different sizes. On the other hand, DMC interestingly crystallized in a botryoidal habit, which is commonly encountered in minerals such as aragonite [25] and has not been reported for DMC.

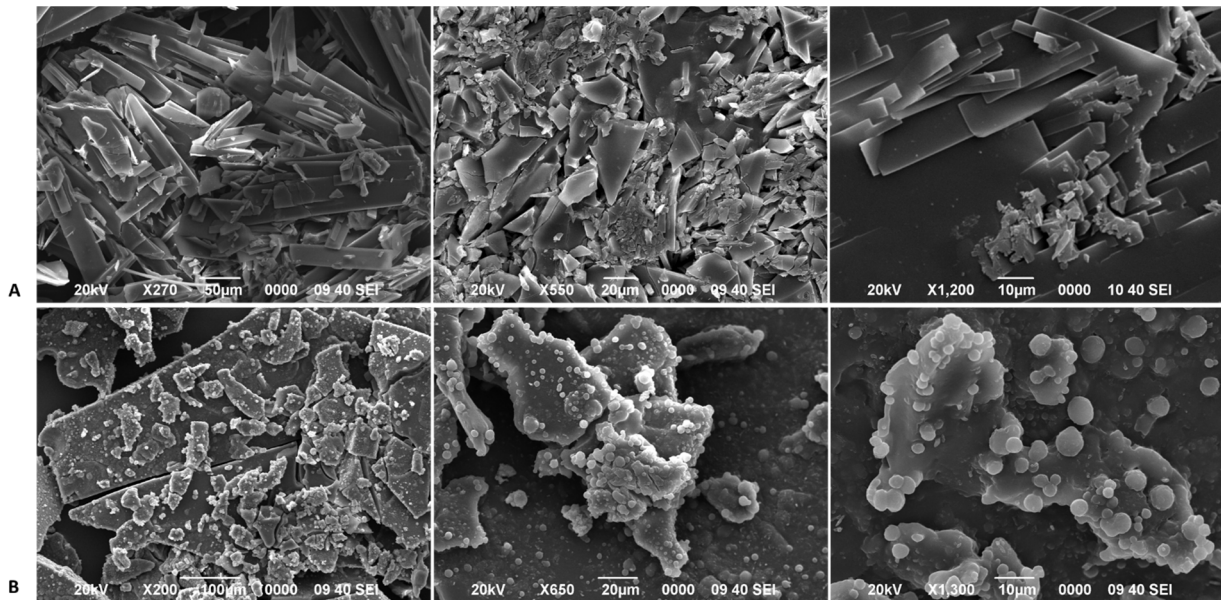


Figure 6. SEM images at different magnifications: (A) BDM at 270×, 550×, and 1200×, and (B) DMC at 200×, 650×, and 1300×.

3.3. In Vitro Studies

3.3.1. Powder Dissolution Test

The powder dissolution profiles of BDM and DMC in both dissolution media are presented in Figure 7. As expected, taking into account the poor water solubility of curcuminoids, the maximum percentage of curcuminoid dissolved was 6% for BDM and around 3% for DMC after 120 min of analysis, related to BDM’s slightly higher aqueous solubility [26].

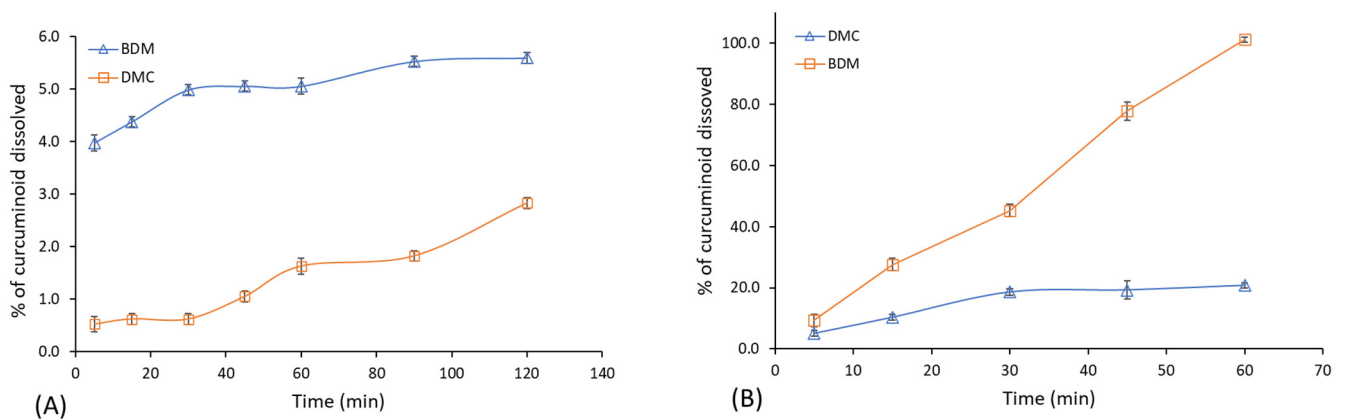


Figure 7. Powder dissolution profiles of BDM and DMC in two dissolution media: (A) water (pH 6.8) and (B) phosphate-buffered saline (pH 7.4). Error bars represent the standard deviation of DMC and BDM concentrations in the triplicates.

Opposite behavior was observed in the buffered medium, in which 100% of the DMC dissolved while BDM achieved around 20% in 1 h. This difference in favor of DMC can be attributed to the different pKa values (DMC < BDM), that can destabilize the keto-enol arrangement and subsequently the dissociation of the enol hydrogen, affecting the stability, and thus the solubility, of the curcuminoids [27].

As reported previously, different media and pH values were evaluated to obtain a reliable dissolution profile of these two curcuminoids. However, anomalous results were observed that have been attributed to the chemical instability of BDM and DMC at pHs lower than 7. In this regard, reports in the literature supported the use of a pH below 7 in the release of curcuminoids [28–30]; and considering the absorption pH in the lumen of the intestine ranges from 6.8 to 7.4, this dissolution media is considered appropriate for curcuminoid evaluation [31].

3.3.2. DPPH Radical-Scavenging Activity

The capacity of scavenging free radicals for these compounds can be adequately evaluated, as described in the literature, by the reaction with a stable free radical, for instance, DPPH [32]. Kinetic studies performed for this test have demonstrated that the rate-determining step involves a fast electron transfer from phenoxide anions to DPPH, following an electron transfer mechanism in protic organic solvents [33]. The antioxidant activity of DMC and BDM was evaluated through the DPPH assay employing EtOH as solvent, as explained in the Materials and Methods subsection. Evaluation of the antioxidant activity indicated that DMC yielded the lowest IC₅₀ (12.46 ± 0.02) µg/mL, with an antioxidant activity 28% higher than the antioxidant activity of BDM, with an IC₅₀ of 17.94 ± 0.06 µg/mL. This result is consistent with the trend reported earlier for the antioxidant activity of these three main curcuminoids, where a good relationship was obtained for the antioxidant values using this DPPH radical method, with CUR having the highest antioxidant value, followed by DMC, that in turn attained a higher antioxidant value than BDM [34].

3.3.3. Cytotoxic Activity Evaluation on Tumoral Cells of DMC and BDM

The *in vitro* cytotoxicity of isolated DMC and BDM were evaluated through the MTT assay using three human tumoral cell lines: gastric adenocarcinoma (AGS), colorectal adenocarcinoma (SW-620), and hepatocellular carcinoma (HepG2). The inhibitory activities (IC₅₀) are presented in Table 4.

Table 4. Cytotoxic activity of curcuminoids in tumoral cell lines.

Cell Line	DMC	BDM
	IC ₅₀ µM (µg/mL)	IC ₅₀ µM (µg/mL)
AGS	52.2 ± 1.4 ^a (17.6 ± 0.5)	57.2 ± 2.5 ^a (17.6 ± 0.8)
SW-620	42.9 ± 2.4 ^a (14.5 ± 0.8)	52.5 ± 0.1 ^a (16.2 ± 0.1)
HepG2	115.6 ± 8.0 ^a (39.1 ± 2.7)	64.7 ± 0.8 ^b (19.9 ± 0.2)
Vero	126.9 ± 5.3 ^a (42.9 ± 1.8)	134.7 ± 5.3 ^a (41.5 ± 1.6)

Values are expressed as mean ± standard deviation (n = 3). In the same row, values with different superscript letters are significantly different at *p* < 0.05.

The cytotoxicity values of both curcuminoids demonstrated a greater effect against colorectal adenocarcinoma cells followed by the effect against the gastric adenocarcinoma cells, and showed a lower effect on hepatic adenocarcinoma cells. According to Mahavorasirikul (2010), for natural product extracts IC₅₀ values lower than 20 µg/mL could be considered of interest for their therapeutic potential [35]. All values shown in Table 4 exhibited better cytotoxic activity than that threshold with the exception of DMC's cytotoxic effect on HepG2 adenocarcinoma cells.

Regarding SW-620 colorectal adenocarcinoma cells, the best cytotoxic effect observed corresponds to the cytotoxic activity of DMC, with an IC₅₀ value of 42.9 µM. The literature

mostly contains reports for CUR, with values of 16 μM [36] and 10 μM [37], achieving a cytotoxic effect higher than 50% in SW-620. Other reports are available for CUR in different colon tumoral cells, for instance IC_{50} for HCT-116 cells was 50 μM [38], 13.9 μM for HCT-15 cells [39], and 9.83 μM for DLD-1 cells [40]. For HT-29 cells the IC_{50} reported for CUR was 40.7 μM [41]. For comparison, isolated CUR was also evaluated in this work, showing an IC_{50} value of $23.1 \pm 1.4 \mu\text{M}$ ($8.5 \pm 0.6 \mu\text{g/mL}$) on SW-620 cells, thus comparable with the other reports. In respect to BDM and DMC, cytotoxicity reports are only available for other colon tumoral cells. For instance, a report on DLD-1 human cells showed IC_{50} values of 8.39 μM and 1.9 μM , respectively [40].

Cytotoxic activity in gastric adenocarcinoma cells (AGS), summarized in Table 4, shows an IC_{50} of 52.1 μM for DMC and 57.2 μM for BDM. The IC_{50} value for the CUR isolated in this study for comparison amounted to 32.5 μM , while for BDM and DMC there are no previous reports for gastric adenocarcinoma cell lines while previous reports in gastric tumoral cell lines showed an IC_{50} of 21.9 μM in AGS cells treated with curcumin [41].

For hepatocellular carcinoma cells, the curcuminoids BDM and DMC presented IC_{50} 's of 64.7 μM and 115.6 μM , respectively (Table 4). Sahu et al. (2016) reported a lower cytotoxic activity ($\text{IC}_{50} = 50 \mu\text{M}$) for CUR in the same HepG2 cell line [38]. In turn, the value obtained in this study for CUR was better, corresponding to an IC_{50} of 40.2 μM .

The mechanisms associated with the cytotoxic effect of curcuminoids have been evaluated in some tumoral cell lines. CUR has been associated with apoptotic induction through activation of the caspase cascade, induction of DNA fragmentation, and inhibition of cytoprotective proteins, such as Bcl₂ [42,43]. CUR was reported to also cause cell cycle arrest through a G1/S block [44]. In turn, DMC has been associated with a modulation of the tumor metastatic process through a binding inhibition of nuclear factor kappa B (NF- κ B) to DNA, which results in a reduced expression of intracellular adhesion molecules such as ICAM-1 and chemokine receptor 4 (CXCR4) [45].

The cytotoxicity of the samples was also assessed in kidney non-tumoral cells (Vero) as a reference for their selectivity between non-tumoral and tumoral cells (selectivity index, SI). BDM presented the highest SI value of 2.6 for SW-620 cells and DMC exhibited the highest SI value of 3.0, while also displaying the best cytotoxic effect against the colon adenocarcinoma cells, showing therefore, in addition a high selectivity against SW-620 cells compared to non-tumoral cells (Table 5). This selectivity is an important parameter to be considered because it suggests a more effective and safe therapeutic potential.

Table 5. Selectivity index of curcuminoids in tumoral cell lines.

Cell Line	DMC	BDM
AGS	2.4	2.4
SW-620	3.0	2.6
HepG2	1.1	2.1

SI: ratio of IC_{50} values of non-tumor cells to cancer cells.

An additional promising aspect of the SI values of DMC and BDM samples is the greater selectivity compared to reference compounds with anticancer activity, such as doxorubicin and cisplatin, for which the SI values are lower, corresponding to 1.0 and 0.9, respectively, in the SW-620 tumoral cell line [46].

4. Conclusions

DMC and BDM were successfully isolated, identified, and characterized. Both solid compounds were shown to be crystalline with an amorphous component, which was higher in BDM, which in turn exhibited a well-defined and faceted prismatic-like crystal shape, while DMC interestingly crystallized in a botryoidal habit not commonly reported in organic materials. The dissolution profile confirmed BDM's slightly higher aqueous solubility with respect to DMC; meanwhile in the buffered medium DMC showed faster dissolution than BDM. Regarding antioxidant activity, DMC yielded an IC_{50} 28% higher

than BDM. Finally, in respect to the cytotoxic effects, DMC showed better IC₅₀ values than BDM towards SW-620 cells (42.9 μM) and AGS cells (52.2 μM), while BDM presented a better IC₅₀ value than DMC on HepG2 cells (64.7 μM). Concerning selectivity, both the compounds BDM and DMC exhibited the highest SI values for SW-620 cells (2.6 and 3.0 respectively) when compared to non-tumoral cells while also displaying the best cytotoxic effect on these colon adenocarcinoma SW-620 cell lines. In sum, the present study results indicate that BDM and DMC deserve further study as potential chemotherapeutic drugs.

Author Contributions: Conceptualization, A.M.A.-S. and M.N.-H.; methodology, A.M.A.-S., F.V.-H., M.N.-H., S.Q. and G.A.; formal analysis, A.M.A.-S., F.V.-H., S.Q. and G.A.; investigation, A.M.A.-S., F.V.-H., M.N.-H., S.Q., G.A. and M.N.-H.; resources, J.R.V.-B., M.N.-H. and A.M.A.-S.; data curation, A.M.A.-S., F.V.-H., S.Q. and G.A.; writing—original draft preparation, A.M.A.-S., F.V.-H., S.Q., G.A. and M.N.-H.; writing—review and editing, J.R.V.-B., M.N.-H. and A.M.A.-S.; supervision, A.M.A.-S., J.R.V.-B. and M.N.-H.; project administration, A.M.A.-S. and M.N.-H.; funding acquisition, J.R.V.-B., M.N.-H. and A.M.A.-S. All authors have read and agreed to the published version of the manuscript.

Funding: This research was partially funded by grants 115-C1-515 and 115-C3-005 from the University of Costa Rica (UCR) and Promotora Costarricense de Innovación e Investigación—MICITT grant number FI-0002-2022.

Institutional Review Board Statement: Not applicable.

Informed Consent Statement: Not applicable.

Data Availability Statement: The data presented in this study are available upon request from the corresponding author.

Acknowledgments: The authors thank the National Laboratory of Nanotechnology (LANOTEC), the University of Costa Rica, and the Research and Extension Center in Materials Engineering (CIEMTEC) of the Costa Rica Institute of Technology (TEC) for the PXRD analyses.

Conflicts of Interest: The authors declare no conflicts of interest.

References

1. Iglesias, J.; Medina, I.; Pazos, M. Galloylation and Polymerization: Role of Structure to Antioxidant Activity of Polyphenols in Lipid Systems. In *Polyphenols in Human Health and Disease*; Academic Press: Cambridge, MA, USA, 2018; p. 1488.
2. Heffernan, C.; Ukrainczyk, M.; Gamidi, R.K.; Hodnett, B.K.; Rasmuson, Å.C. Extraction and Purification of Curcuminoids from Crude Curcumin by a Combination of Crystallization and Chromatography. *Org. Process Res. Dev.* **2017**, *21*, 821–826. [[CrossRef](#)]
3. Ukrainczyk, M.; Hodnett, B.K.; Rasmuson, Å.C. Process Parameters in the Purification of Curcumin by Cooling Crystallization. *Org. Process Res. Dev.* **2016**, *20*, 1593–1602. [[CrossRef](#)]
4. Nair, A.; Amalraj, A.; Jacob, J.; Kunnumakkara, A.B.; Gopi, S. Non-curcuminoids from turmeric and their potential in cancer therapy and anticancer drug delivery formulations. *Biomolecules* **2019**, *9*, 13. [[CrossRef](#)] [[PubMed](#)]
5. Aggarwal, B.B.; Harikumar, K.B. Potential therapeutic effects of curcumin, the anti-inflammatory agent, against neurodegenerative, cardiovascular, pulmonary, metabolic, autoimmune and neoplastic diseases. *Int. J. Biochem. Cell Biol.* **2009**, *41*, 40–59. [[CrossRef](#)] [[PubMed](#)]
6. Aron, P.M.; Kennedy, J.A. Flavan-3-ols: Nature, occurrence and biological activity. *Mol. Nutr. Food Res.* **2008**, *52*, 79–104. [[CrossRef](#)] [[PubMed](#)]
7. Aggarwal, B.B.; Gupta, S.C.; Sung, B. Curcumin: An orally bioavailable blocker of TNF and other pro-inflammatory biomarkers. *Br. J. Pharmacol.* **2013**, *169*, 1672–1692. [[CrossRef](#)]
8. Jin, C.Y.; Lee, J.D.; Park, C.; Choi, Y.H.; Kim, G.Y. Curcumin attenuates the release of pro-inflammatory cytokines in lipopolysaccharide-stimulated BV2 microglia. *Acta Pharmacol. Sin.* **2007**, *28*, 1645–1651. [[CrossRef](#)]
9. Rahardjo, B.; Widjajanto, E.; Sujuti, H.; Keman, K. Curcumin decreased level of proinflammatory cytokines in monocyte cultures exposed to preeclamptic plasma by affecting the transcription factors NF-κB and PPAR-γ. *Biomark. Genom. Med.* **2014**, *6*, 105–115. [[CrossRef](#)]
10. Liu, J.; Wang, Q.; Omari-Siaw, E.; Adu-Frimpong, M.; Liu, J.; Xu, X.; Yu, J. Enhanced oral bioavailability of Bisdemethoxycurcumin-loaded self-microemulsifying drug delivery system: Formulation design, in vitro and in vivo evaluation. *Int. J. Pharm.* **2020**, *590*, 119887. [[CrossRef](#)]
11. Guo, L.Y.; Cai, X.F.; Lee, J.J.; Kang, S.S.; Shin, E.M.; Zhou, H.Y.; Jung, J.W.; Kim, Y.S. Comparison of suppressive effects of demethoxycurcumin and bisdemethoxycurcumin on expressions of inflammatory mediators In Vitro and In Vivo. *Arch. Pharm. Res.* **2008**, *31*, 490–496. [[CrossRef](#)]

12. Ponnusamy, L.; Natarajan, S.R.; Thangaraj, K.; Manoharan, R. Therapeutic aspects of AMPK in breast cancer: Progress, challenges, and future directions. *Biochim. Biophys. Acta-Rev. Cancer* **2020**, *1874*, 188379. [[CrossRef](#)] [[PubMed](#)]
13. Yodkeeree, S.; Chaiwangyen, W.; Garbisa, S.; Limtrakul, P. Curcumin, demethoxycurcumin and bisdemethoxycurcumin differentially inhibit cancer cell invasion through the down-regulation of MMPs and uPA. *J. Nutr. Biochem.* **2009**, *20*, 87–95. [[CrossRef](#)] [[PubMed](#)]
14. Hassanzadeh, K.; Buccarello, L.; Dragotto, J.; Mohammadi, A.; Corbo, M.; Feligioni, M. Obstacles against the Marketing of Curcumin as a Drug. *Int. J. Mol. Sci.* **2020**, *21*, 6619. [[CrossRef](#)] [[PubMed](#)]
15. Liu, W.; Xian, J.; Wang, J.; Huang, J.; Xu, Z. Pharmacokinetic Characteristics of Bisdemethoxycurcumin and Its Mechanism of Reversing Cardiomyocyte Apoptosis. *Indian J. Pharm. Sci.* **2023**, *85*, 64–73. [[CrossRef](#)]
16. Huang, C.; Lu, H.-F.; Chen, Y.-H.; Chen, J.-C.; Chou, W.-H.; Huang, H.-C. Curcumin, demethoxycurcumin, and bisdemethoxycurcumin induced caspase-dependent and -independent apoptosis via Smad or Akt signaling pathways in HOS cells. *BMC Complement. Med. Ther.* **2020**, *20*, 68. [[CrossRef](#)] [[PubMed](#)]
17. Quirós-Fallas, M.I.; Vargas-Huertas, F.; Quesada-Mora, S.; Azofoifa-Cordero, G.; Wilhelm-Romero, K.; Vásquez-Castro, F.; Alvarado-Corella, D.; Sánchez-Kopper, A.; Navarro-Hoyos, M. Polyphenolic HRMS Characterization, Contents and Antioxidant Activity of *Curcuma longa* Rhizomes from Costa Rica. *Antioxidants* **2022**, *11*, 620. [[CrossRef](#)]
18. Jayaprakasha, G.K.; Nagana Gowda, G.A.; Marquez, S.; Patil, B.S. Rapid separation and quantitation of curcuminoids combining pseudo two-dimensional liquid flash chromatography and NMR spectroscopy. *J. Chromatogr. B* **2013**, *937*, 25–32. [[CrossRef](#)]
19. Payton, F.; Sandusky, P.; Alworth, W.L. NMR Study of the Solution Structure of Curcumin. *J. Nat. Prod.* **2007**, *70*, 143–146. [[CrossRef](#)]
20. Prasad, D.; Praveen, A.; Mahapatra, S.; Mogurampelly, S.; Chaudhari, S.R. Existence of β -diketone form of curcuminoids revealed by NMR spectroscopy. *Food Chem.* **2021**, *360*, 130000. [[CrossRef](#)]
21. Yuan, L.; Horosanskaia, E.; Engelhardt, F.; Edelmann, F.T.; Couvrat, N.; Sanselme, M.; Cartigny, Y.; Coquerel, G.; Seidel-Morgenstern, A.; Lorenz, H. Solvate Formation of Bis(demethoxy)curcumin: Crystal Structure Analyses and Stability Investigations. *Cryst. Growth Des.* **2019**, *19*, 854–867. [[CrossRef](#)]
22. Wünsche, S.; Yuan, L.; Seidel-Morgenstern, A.; Lorenz, H. A Contribution to the Solid State Forms of Bis(demethoxy)curcumin: Co-Crystal Screening and Characterization. *Molecules* **2021**, *26*, 720. [[CrossRef](#)] [[PubMed](#)]
23. Gunasekaran, S.; Natarajan, R.K.; Natarajan, S.; Rathikha, R. Structural investigation on curcumin. *Asian J. Chem.* **2008**, *20*, 2903–2913.
24. Péret-Almeida, L.; Cherubino, A.P.F.; Alves, R.J.; Dufossé, L.; Glória, M.B.A. Separation and determination of the physico-chemical characteristics of curcumin, demethoxycurcumin and bisdemethoxycurcumin. *Food Res. Int.* **2005**, *38*, 1039–1044. [[CrossRef](#)]
25. Ge, Y.; Della Porta, G.; Pederson, C.L.; Lokier, S.W.; Hoffmann, R.; Immenhauser, A. Botryoidal and Spherulitic Aragonite in Carbonates Associated with Microbial Mats: Precipitation or Diagenetic Replacement Product? *Front. Earth Sci.* **2021**, *9*, 698952. [[CrossRef](#)]
26. Lateh, L.; Kaewnopparat, N.; Yuenyongsawad, S.; Panichayupakaranant, P. Enhancing the water-solubility of curcuminoids-rich extract using a ternary inclusion complex system: Preparation, characterization, and anti-cancer activity. *Food Chem.* **2022**, *368*, 130827. [[CrossRef](#)]
27. D'Archivio, A.A.; Maggi, M.A. Investigation by response surface methodology of the combined effect of pH and composition of water-methanol mixtures on the stability of curcuminoids. *Food Chem.* **2017**, *219*, 414–418. [[CrossRef](#)]
28. Kharat, M.; Du, Z.; Zhang, G.; McClements, D.J. Physical and Chemical Stability of Curcumin in Aqueous Solutions and Emulsions: Impact of pH, Temperature, and Molecular Environment. *J. Agric. Food Chem.* **2017**, *65*, 1525–1532. [[CrossRef](#)]
29. Xie, X.; Tao, Q.; Zou, Y.; Zhang, F.; Guo, M.; Wang, Y.; Wang, H.; Zhou, Q.; Yu, S. PLGA Nanoparticles Improve the Oral Bioavailability of Curcumin in Rats: Characterizations and Mechanisms. *J. Agric. Food Chem.* **2011**, *59*, 9280–9289. [[CrossRef](#)]
30. Prajakta, D.; Ratnesh, J.; Chandan, K.; Suresh, S.; Grace, S.; Meera, V.; Vandana, P. Curcumin Loaded pH-Sensitive Nanoparticles for the Treatment of Colon Cancer. *J. Biomed. Nanotechnol.* **2009**, *5*, 445–455. [[CrossRef](#)]
31. Baek, J.-S.; Cho, C.-W. Surface modification of solid lipid nanoparticles for oral delivery of curcumin: Improvement of bioavailability through enhanced cellular uptake, and lymphatic uptake. *Eur. J. Pharm. Biopharm.* **2017**, *117*, 132–140. [[CrossRef](#)]
32. Niki, E. Antioxidant Capacity: Which Capacity and How to Assess It? *J. Berry Res.* **2011**, *1*, 169–176. [[CrossRef](#)]
33. Foti, M.; Daquino, C.; Geraci, C. Electron-Transfer Reaction of Cinnamic Acids and Their Methyl Esters with the DPPH_• Radical in Alcoholic Solutions. *J. Org. Chem.* **2004**, *69*, 2309–2314. [[CrossRef](#)] [[PubMed](#)]
34. Jayaprakasha, G.K.; Jaganmohan Rao, L.; Sakariah, K.K. Antioxidant activities of curcumin, demethoxycurcumin and bisdemethoxycurcumin. *Food Chem.* **2006**, *98*, 720–724. [[CrossRef](#)]
35. Mahavorasirikul, W.; Viyanant, V.; Chaijaroenkul, W.; Itharat, A.; Na-Bangchang, K. Cytotoxic activity of Thai medicinal plants against human cholangiocarcinoma, laryngeal and hepatocarcinoma cells in vitro. *BMC Complement. Altern. Med.* **2010**, *10*, 55. [[CrossRef](#)] [[PubMed](#)]
36. Jiang, X.; Li, S.; Qiu, X.; Cong, J.; Zhou, J.; Miu, W. Curcumin Inhibits Cell Viability and Increases Apoptosis of SW620 Human Colon Adenocarcinoma Cells via the Caudal Type Homeobox-2 (CDX2)/Wnt/ β -Catenin Pathway. *Med. Sci. Monit.* **2019**, *25*, 7451–7458. [[CrossRef](#)] [[PubMed](#)]
37. Han, X.; Guo, L.; Jiang, X.; Wang, Y.; Wang, Z.; Li, D. Curcumin Inhibits Cell Viability by Inducing Apoptosis and Autophagy in Human Colon Cancer Cells. *Proc. Anticancer Res.* **2019**, *3*, 133180. [[CrossRef](#)]

38. Sahu, P.K.; Sahu, P.K.; Sahu, P.L.; Agarwal, D.D. Structure activity relationship, cytotoxicity and evaluation of antioxidant activity of curcumin derivatives. *Bioorg. Med. Chem. Lett.* **2016**, *26*, 1342–1347. [[CrossRef](#)]
39. Lozada-García, M.C.; Enríquez, R.G.; Ramírez-Apán, T.O.; Nieto-Camacho, A.; Palacios-Espinosa, J.F.; Custodio-Galván, Z.; Soria-Arteche, O.; Pérez-Villanueva, J. Synthesis of curcuminoids and evaluation of their cytotoxic and antioxidant properties. *Molecules* **2017**, *22*, 633. [[CrossRef](#)]
40. Adeyeni, T.A.; Khatwani, N.; San, K.; Ezekiel, U.R. BMI1 is downregulated by the natural compound curcumin, but not by bisdemethoxycurcumin and dimethoxycurcumin. *Physiol. Rep.* **2016**, *4*, e12906. [[CrossRef](#)]
41. Cao, A.; Li, Q.; Yin, P.; Dong, Y.; Shi, H.; Wang, L.; Ji, G.; Xie, J.; Wu, D. Curcumin induces apoptosis in human gastric carcinoma AGS cells and colon carcinoma HT-29 cells through mitochondrial dysfunction and endoplasmic reticulum stress. *Apoptosis* **2013**, *18*, 1391–1402. [[CrossRef](#)]
42. Huang, T.-Y.; Hsu, C.-W.; Chang, W.-C.; Wang, M.-Y.; Wu, J.-F.; Hsu, Y.-C. Demethoxycurcumin Retards Cell Growth and Induces Apoptosis in Human Brain Malignant Glioma GBM 8401 Cells. *Evid.-Based Complement. Altern. Med.* **2012**, *2012*, 396573. [[CrossRef](#)] [[PubMed](#)]
43. Lee, P.; Woo, S.; Jee, J.-G.; Sung, S.; Kim, H. Bisdemethoxycurcumin Induces Apoptosis in Activated Hepatic Stellate Cells via Cannabinoid Receptor 2. *Molecules* **2015**, *20*, 1277–1292. [[CrossRef](#)] [[PubMed](#)]
44. Basile, V.; Ferrari, E.; Lazzari, S.; Belluti, S.; Pignedoli, F.; Imbriano, C. Curcumin derivatives: Molecular basis of their anti-cancer activity. *Biochem. Pharmacol.* **2009**, *78*, 1305–1315. [[CrossRef](#)] [[PubMed](#)]
45. Yodkeeree, S.; Ampasavate, C.; Sung, B.; Aggarwal, B.B.; Limtrakul, P. Demethoxycurcumin suppresses migration and invasion of MDA-MB-231 human breast cancer cell line. *Eur. J. Pharmacol.* **2010**, *627*, 8–15. [[CrossRef](#)]
46. Strzyga-Łach, P.; Chrzanowska, A.; Podsadni, K.; Bielenica, A. Investigation of the Mechanisms of Cytotoxic Activity of 1,3-Disubstituted Thiourea Derivatives. *Pharmaceuticals* **2021**, *14*, 1097. [[CrossRef](#)]

Disclaimer/Publisher’s Note: The statements, opinions and data contained in all publications are solely those of the individual author(s) and contributor(s) and not of MDPI and/or the editor(s). MDPI and/or the editor(s) disclaim responsibility for any injury to people or property resulting from any ideas, methods, instructions or products referred to in the content.